1661-8726/08/01S111-16
DOI 10.1007/s00015-008-1290-0
Birkhäuser Verlag, Basel, 2008

Swiss J. Geosci. 101 (2008) Supplement 1, S111–S126

The metamorphic evolution of migmatites from the Ötztal Complex (Tyrol, Austria) and constraints on the timing of the pre-Variscan high-T event in the Eastern Alps

Werner F. Thöny *, [1], Peter Tropper [1], Friederike Schennach [1], Erwin Krenn [2], Friedrich Finger [2], Reinhard Kaindl [1], Franz Bernhard [3] & Georg Hoinkes [3]

Key words: pre-Variscan, high-T, migmatite, monazite, geochronolgy, Eastern Alps

ABSTRACT

Within the Ötztal Complex (ÖC), migmatites are the only geological evidence of the pre-Variscan metamorphic evolution, which led to the occurrence of partial anatexis in different areas of the complex. We investigated migmatites from three localities in the ÖC, the Winnebach migmatite in the central part and the Verpeil- and Nauderer Gaisloch migmatite in the western part. We determined metamorphic stages using textural relations and electron microprobe analyses. Furthermore, chemical microprobe ages of monazites were obtained in order to associate the inferred stages of mineral growth to metamorphic events. All three migmatites show evidence for a polymetamorphic evolution (pre-Variscan, Variscan) and only the Winnebach migmatite shows evidence for a P-accentuated Eo-Alpine metamorphic overprint in the central ÖC. The P-T data range from 670–750 °C and <2.8 kbar for the pre-Variscan event, 550–650 °C and 4–7 kbar for the Variscan event and 430–490 °C and ca. 8.5 kbar for the P-accentuated Eo-Alpine metamorphic overprint. U-Th-Pb electron microprobe dating of monazites from the leucosomes from all three migmatites provides an average age of 441 ± 18 Ma, thus indicating a pervasive Ordovician-Silurian metamorphic event in the ÖC.

Introduction

Polymetamorphic crystalline complexes provide a window into the metamorphic evolution of large-scale orogenic belts, such as the Alps. Deciphering the metamorphic history by means of petrographic, mineral chemical and geochronological data will help to unravel the geodynamic evolution of these belts and increase our knowledge and understanding of large-scale orogenic processes. Due to the mineralogical and textural complexities in polymetamorphic rocks, it is imperative to apply advanced analytical techniques with high spatial resolution to obtain reliable information on the P-T-t path.

The Austroalpine Ötztal Complex (ÖC) in the Eastern Alps provides an excellent opportunity to study a metamorphic complex which underwent several episodes of metamorphic overprint. Although extensive research has been performed on the two predominant orogenic episodes in the Eastern Alps, namely the Variscan (Hercynian) and Eo-Alpine orogenic events, very little attention has been paid to the pre-Variscan metamorphic history so far. Compared to the Variscan and Eo-Alpine events, which can be traced throughout the whole ÖC, the pre-Variscan history is manifested only in localized migmatite occurrences within the ÖC. Thus these migmatites provide the opportunity to study polymetamorphic rocks that underwent at least three metamorphic episodes (Neubauer et al. 1999; Hoinkes et al. 1999). Within the ÖC, several migmatite occurrences were described from the Ötz valley, the Kauner valley, the Reschenpass area and the Stubai valley (Schindlmayer 1999). We will focus our investigations on three migmatite bodies. Two of these migmatite bodies were only recently discovered, the Verpeil migmatite and the migmatite from the Nauderer Gaisloch (Schweigl 1993; Bernhard 1994) and of these two, only the latter was studied to some extent petrographically and geochronologically (Klötzli-Chowanetz 2001). The third is the Winnebach migmatite from the central ÖC, but despite of its relatively large size (25 km^2) and importance as a locality to study the pre-Variscan metamorphic history, only limited information on its petrology and mineral chemistry is available (e.g. Hoinkes et al. 1972; Hoinkes 1973; Klötzli-Chowanetz 2001). Although the electron microprobe has been the major tool to perform micro-analytical techniques at small scales over the last thirty years, only very few mineral chemical data are avail-

[1]University of Innsbruck, Faculty of Geo- and Atmospheric Sciences, Institute of Mineralogy and Petrography, Innrain 52, A-6020 Innsbruck, Austria.
[2]University of Salzburg, Department of Material Sciences, Division of Mineralogy, Hellbrunnerstr. 34, A-5020 Salzburg, Austria.
[3]University of Graz, Institute of Geo Sciences, Division of Mineralogy and Petrography, Universitätsplatz 2, A-8010 Graz, Austria.
*Corresponding author: Werner Thöny. E-mail: Werner.Thoeny@uibk.ac.at

able from these migmatites. The lack of basic chemical data thus prevents an application of modern thermobarometric and geochronological techniques to resolve the P-T-t history of these rocks.

High-grade metamorphic pelitic rocks also provide an excellent opportunity for monazite dating using the electron microprobe analyser (EMPA) (e.g. Finger et al. 1996; Finger & Helmy 1998; Goncalves et al. 2004). Since this method is very fast and destruction-free because it can be used in thin sections, it has become one of the most popular dating methods (Finger et al. 1998; Williams et al. 2006; Cocherie et al. 2005). In the Ötztal Complex (ÖC) a large amount of age data concerning the pre-Variscan igneous and metamorphic evolution exists (e.g. Thöni 1999; Neubauer et al. 1999). Geochronological investigations in the ÖC over the last twenty years reveal several stages of emplacement of igneous rocks prior to the dominant Variscan and Eo-Alpine metamorphic episodes (Thöni 1999). The oldest stage involves gabbroic and diorite-tonalitic intrusions with ages between 487 and 540 Ma (Klötzli-Chowanetz 2001; Hoinkes et al. 1997; Miller & Thöni 1995; Schweigl 1993). The majority of intrusives in the central ÖC is granitic in composition and most ages scatter between 420 and 485 Ma (Thöni 1999). The latter ages seem to correlate well with those obtained from zircons from the Winnebach migmatite (490 ± 9 Ma, Klötzli-Chowanetz et al. 1997) and also with Rb-Sr cooling ages of micas (461 ± 4 Ma, Chowanetz 1991) thus placing a time constraint on the formation of the migmatites in the early Ordovician.

Nonetheless, the age of the pre-Variscan migmatization is still ambiguous. Geochronological investigations on the Winnebach migmatite yielded two contrasting ages of the anatexis so far. Söllner & Hansen (1987) and Söllner (2001) obtained Pan-African ages of 607–670 Ma and Klötzli-Chowanetz et al. (1997) obtained ages of the migmatization ranging from 461 ± 4 Ma to 490 ± 9 Ma (Chowanetz 1991; Klötzli-Chowanetz 2001). No age data have been available so far from the Verpeil migmatite body but only of the intrusions that presumably caused the migmatization, namely the metagranitoids surrounding the Verpeil migmatite (408–487 Ma, Bernhard et al. 1996). The available ages for the Nauderer Gaisloch migmatite also yield a wide range from 430 ± 6 Ma to 585 ± 8 (Schweigl 1993; Klötzli-Chowanetz 2001). Therefore, the pervasive character and the lateral extent of these events in the ÖC is still unclear.

The aim of this investigation is to unravel the metamorphic P-T-t evolution of these migmatite bodies with special emphasis on the pre-Variscan metamorphic history of the ÖC. Due to the fact that the vast majority of petrological and geochronological data from the Eastern Alps deal with the Variscan (Neubauer et al. 1999) and Eo-Alpine (Hoinkes et al. 1999) metamorphic events, it is the aim of this work to fill the gap in respect to the pre-Variscan metamorphic history. Due to their polymetamorphic nature, the migmatites provide the unique opportunity to obtain P-T-t data of the pre-Variscan, Variscan and possibly Eo-Alpine events from this portion of the Eastern Alps and therefore truly represent a window into the metamorphic evolution of the Austroalpine basement west of the Tauern Window.

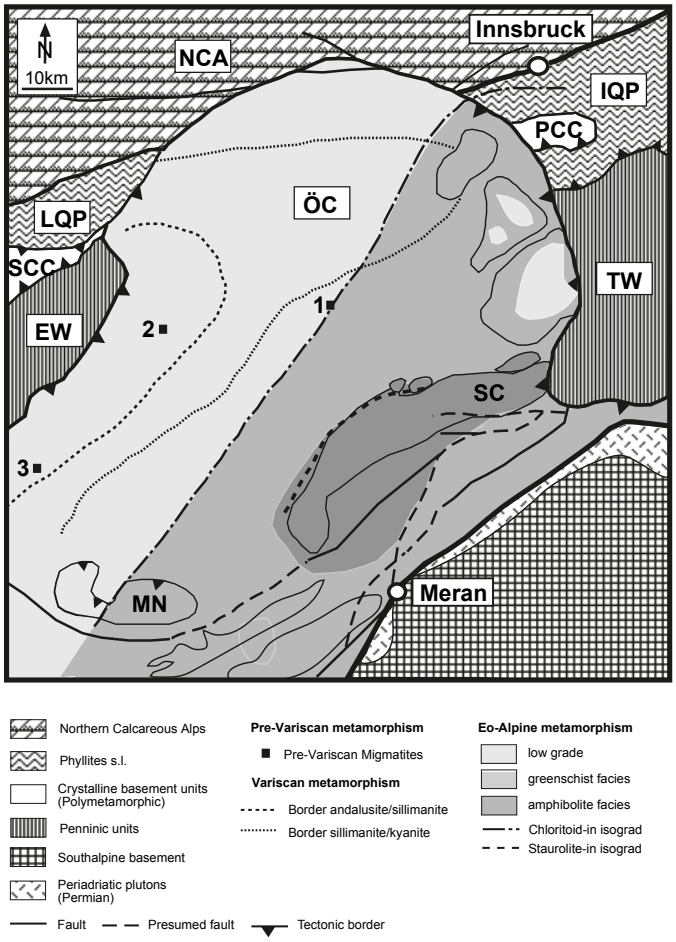

Fig. 1. Schematic tectonic overview of the area west of the Tauern window. The black squares indicate the localities of the migmamtite bodies. 1: Winnebach migmatite, 2: Verpeil migmatite, 3: Nauderer Gaisloch migmatite. NCA = Northern Calcareous Alps, LQP = Landeck Quartzphyllite, IQP = Innsbruck Quartzphyllite, PCC = Patscherkofel Crystalline Complex, TW = Tauern Window, EW = Engadin Window, MN = Matsch Nappe, SC = Schneeberg Complex, SCC = Silvretta Crystalline Complex.

Geological setting and field relations

The three migmatite bodies in the ÖC, which are the focus of this investigation and which formed by partial melting of biotite-plagioclase gneisses and biotite schists, are: (1) the Winnebach migmatite near Längenfeld in the Ötz valley; (2) the Verpeil migmatite in the Kauner valley; (3) and the migmatite body of the Nauderer Gaisloch near the Reschenpass (Fig. 1).

The Winnebach migmatite from the central ÖC has already been recognized as showing features of a magmatic rock at the beginning of the 20th century by Ohnesorge (1905) and Hammer (1925). It mainly consists of granodioritic neosome containing remnants of biotite-plagioclase gneisses and schollen of biotite schists and calc-silicate lenses, thus indicating a

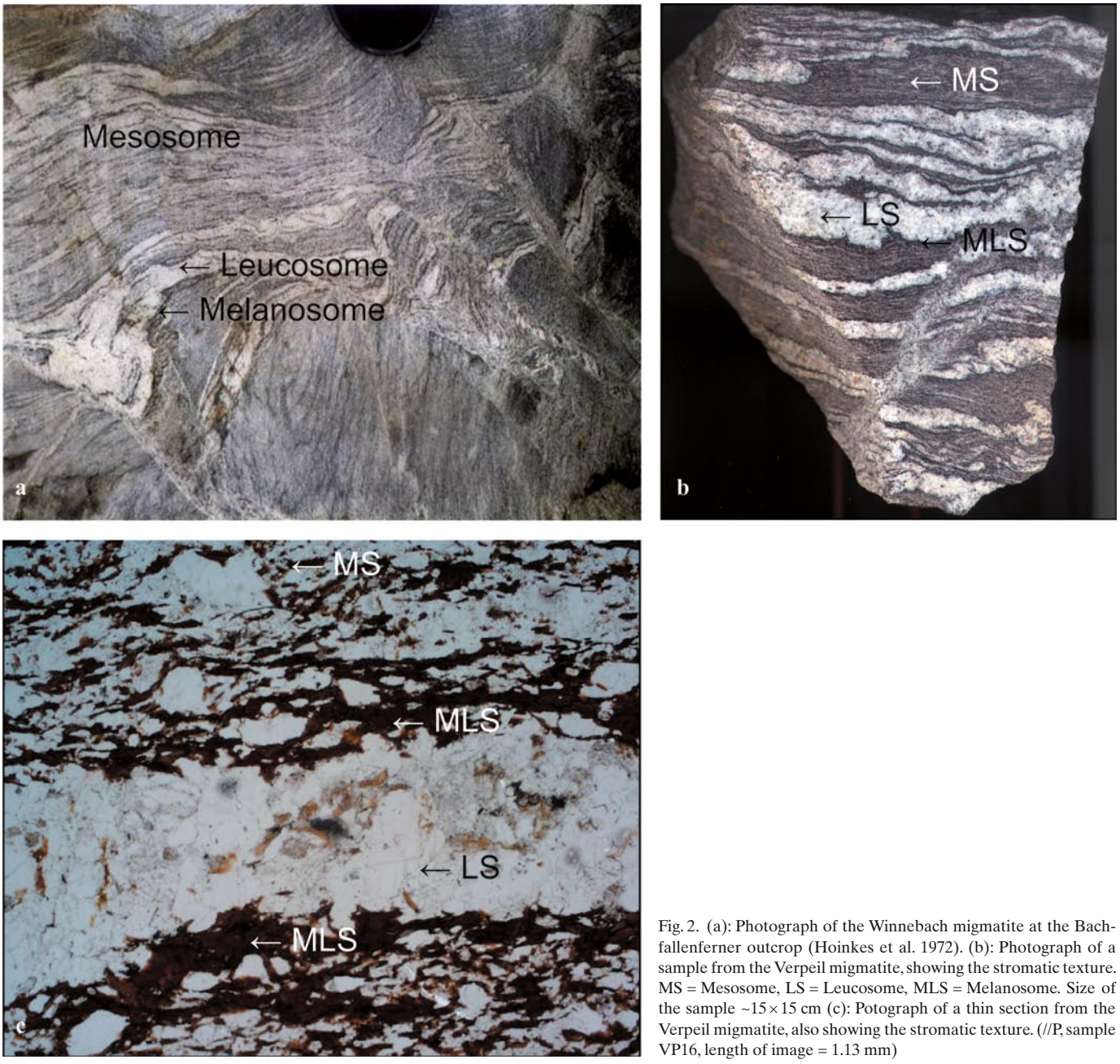

Fig. 2. (a): Photograph of the Winnebach migmatite at the Bachfallenferner outcrop (Hoinkes et al. 1972). (b): Photograph of a sample from the Verpeil migmatite, showing the stromatic texture. MS = Mesosome, LS = Leucosome, MLS = Melanosome. Size of the sample ~15 × 15 cm (c): Potograph of a thin section from the Verpeil migmatite, also showing the stromatic texture. (//P, sample VP16, length of image = 1.13 mm)

higher degree of melting compared to the Verpeil migmatite as shown in Figure 2a (Hoinkes et al. 1972). The migmatite complex contains a central core unaffected by any post-Ordovician metamorphic overprint (Drong 1959; Hoinkes et al. 1972). This undeformed part of the migmatite is the product of in-situ anatexis of biotite-plagioclase paragneisses (Hoinkes et al. 1972; Hoinkes 1973). The other two migmatites, the Verpeil migmatite and the Nauderer Gaisloch migmatite, were only recently found (Schweigl 1993; Bernhard 1994) and almost no data therefore exist. In contrast to the Winnebach migmatite, the Verpeil migmatite and the Nauderer Gaisloch migmatite are stromatic migmatites according to the classification of Mehnert (1968), containing small bands of leucosomes, indicating a relatively small degree around 5 Vol.% of partial melting. The leucosome is surrounded by a thin (ca. 1–2 mm) layer of biotite selvages, which represent the melanosome (Figs. 2b–c). The leucosome layers often show ptygmatic folding.

Petrography and microstructural relations

Migmatites from all three localities contain the minerals plagioclase + muscovite + biotite + quartz + K-feldspar + accessories

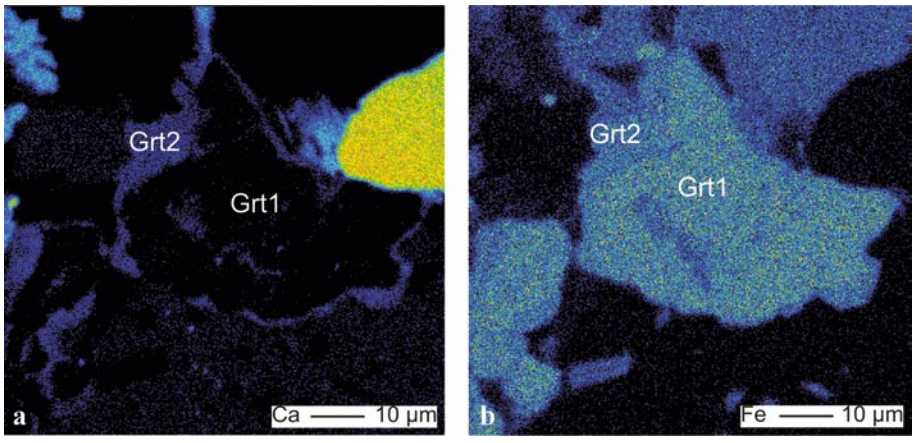

Fig. 3. (a): X-ray distribution image for the element Ca showing two generations of garnet (Grt_1 + Grt_2) from a leucosome sample of the Winnebach migmatite (sample WB 70). Ca is distinctly enriched at the rims. (b): X-ray distribution image for the element Fe also showing the two generations of garnet (Grt_1 + Grt_2) and a decrease in Fe at the rims of the grain.

± garnet ± kyanite ± silimanite ± andalusite ± cordierite. Previous petrographic investigations from the three localities by Hoinkes et al. (1972), Söllner et al. (1982), Chowanetz (1991), Schweigl (1993), Bernhard (1994), and Klötzli-Chowanetz (2001) provided evidence for several stages of mineral growth of plagioclase, biotite and quartz during the metamorphic evolution of these migmatite bodies.

In the Winnebach migmatite, garnet forms hypidiomorphic to idiomorphic grains ranging from 50 to 100 µm in size. Backscatter electron (BSE) images reveal two stages of plagioclase and garnet growth (Figs. 3a-b). Biotite texturally also shows evidence for two generations. Older biotites are large, idiomorphic crystals which are surrounded by fine-grained younger biotites (Fig. 4). Similarly, two generations of kyanite occur (Fig. 5a), which were distinguished by micro-Raman spectroscopy since the younger fine-grained kyanite shows a strongly fluorescing Raman spectrum (Figs. 5b-c). Textures which indicate melting rarely occur (Figs. 6a-c). These textures show a haplogranitic assemblage and indicate melting according to the model reactions (Boettcher & Wyllie 1968; Spear et al. 1999):

Plagioclase + K-feldspar + Biotite + Quartz = Melt (1)

Muscovite + K-feldspar + Quartz + H_2O = Melt (2)

In addition, large pseudomorphs containing muscovite + chlorite are interpreted as pinite pseudomorphs after cordierite. Chloritoid occurs as fine-grained needles along former fractures.

In contrast to the other two migmatites, the Verpeil migmatite still contains relicts of cordierite as shown in Figures 7a–b, which is actually the first report of cordierite from migmatites from the ÖC. These cordierites are partly replaced by kyanite, biotite, and plagioclase (Figs. 7a–c) indicating a reaction such as:

Cordierite + K-feldspar + H_2O = Biotite + Kyanite (3)

Garnet grows around biotite (Fig. 8) and kyanite forms either needle-shaped grains or relict large crystals, surrounded by later formed andalusite (Figs. 9a–b), as identified with Raman spectroscopy (Fig. 9c). In addition, cordierite is also replaced by extremely fine-grained muscovite and chlorite (pinitization), which formed during a later stage.

The mineral assemblage of the Nauderer Gaisloch migmatite is very similar to the one of the Verpeil migmatite and is comprised of garnet + quartz + biotite + plagioclase + muscovite + $kyanite_{1,2}$. $Kyanite_1$ occurs as large grains, and $kyanite_2$ occurs as small needles intergrown with biotite (Fig. 10), which could also have replaced former cordierite according to reaction (3).

Analytical methods

Electron microprobe analysis (EMPA) of all minerals except monazite was performed using the JEOL 8100 SUPERPROBE at the Institute of Mineralogy and Petrography at the University of Innsbruck. Operating conditions were 15 kV acceleration voltage and 20 nA beam current. A defocused beam with a

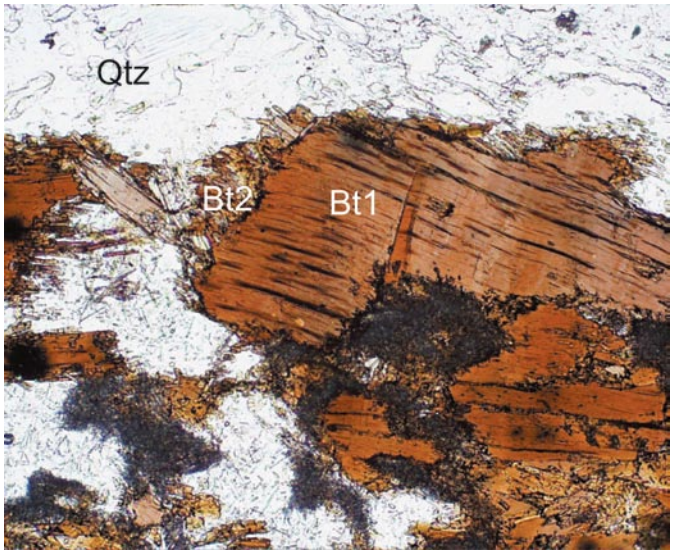

Fig. 4. Photograph of a thin section of sample WB9A2 showing the two, texturally different, generations of biotite. (//P, length of image = 1.13 mm, Bt1 = biotite1, Bt2 = biotite2, Qtz = quartz)

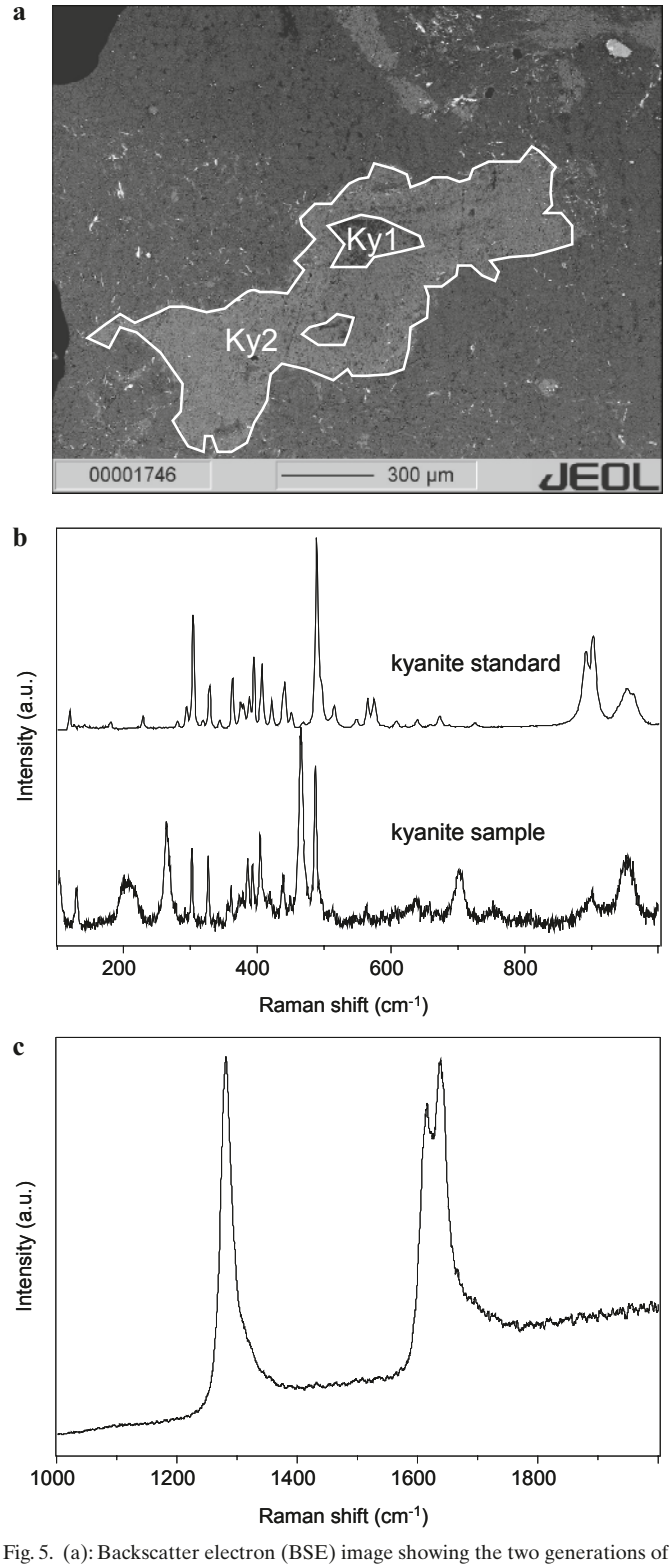

Fig. 5. (a): Backscatter electron (BSE) image showing the two generations of kyanite (Ky_1 + Ky_2) from the Winnebach migmatite (sample WB 70). (b): Raman spectrum of the texturally older $kyanite_1$. The dark grey spectrum is from sample WB9A2, the light grey is a standard kyanite spectrum. The spectrum also includes peaks from adjacent minerals (quartz) and adhesive but clearly identifies the aluminium silicate as kyanite. (c): Raman spectrum of the fluorescing $kyanite_2$ (WB9A2).

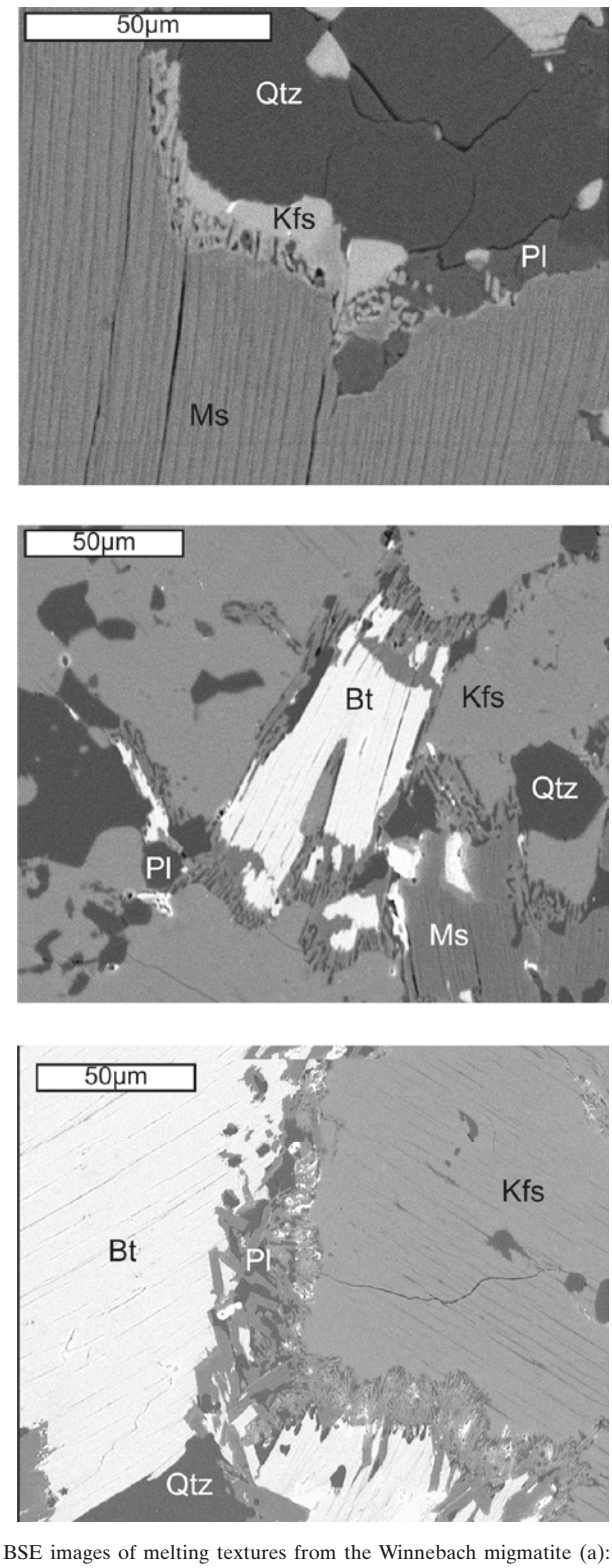

Fig. 6. BSE images of melting textures from the Winnebach migmatite (a): melting textures involving the assemblage plagioclase (Pl) + K-feldspar (Kfs) + muscovite (Ms) + quartz (Qtz) (sample WB9A2). (b): melting textures involving the assemblage biotite (Bt) + muscovite (Ms) + K-feldspar (Kfs) + plagioclase (Pl) + quartz (Qtz) (sample WB9A2). (c): melting textures involving melting of the assemblage biotite (Bt) + K-feldspar (Kfs) + quartz (Qtz) + plagioclase (Pl) (sample WB9A2).

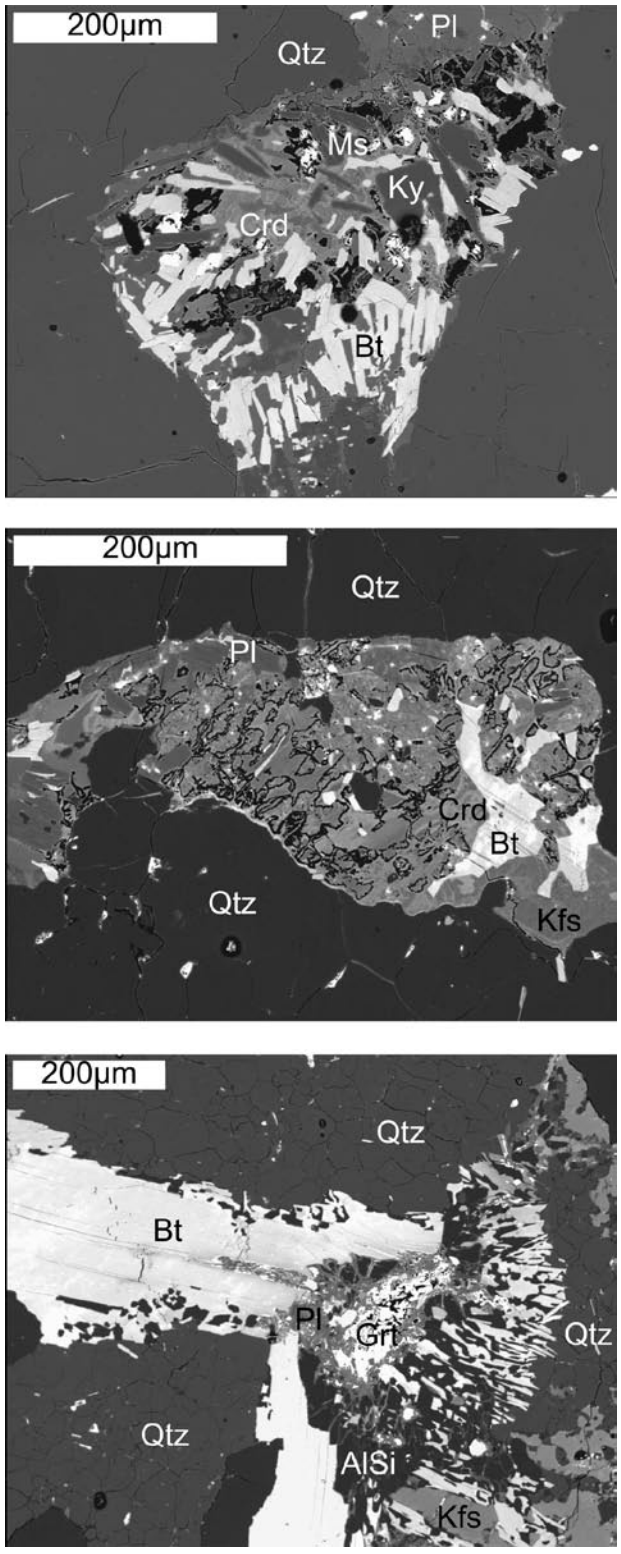

Fig. 7. BSE images of biotite + kyanite pseudomorphs after cordierite from the Verpeil migmatite. Relict cordierite is still present in the samples FB56E and VP16 (a, b). (c): garnet + K-feldspar also occur within the pseudomorphs according to reaction (5). Abbreviations: Crd = cordierite, Bt = biotite, Ky = kyanite, Ms = muscovite, Pl = plagioclase, Qtz = quartz, Grt = garnet, Kfs = K-feldspar, AlSi = aluminium silicate.

diameter of 5 µm was used for the analysis of feldspars and micas to prevent loss of alkalis. Mineral formulae were calculated using the software NORM II (Ulmer 1993, written comm.). Microprobe analyses of monazite were obtained in wavelength dispersive (WD) mode on a JEOL JX 8600 electron microprobe at the University of Salzburg. Operating conditions were 15 kV acceleration voltage, 150–200 nA beam current. Mα lines were chosen for Th, U and Pb; Lβ lines for Pr, Nd, Sm, Eu and Gd; Lα lines for Sr, Y, La, Ce, Dy, Er and Yb and Kα lines for Si, Al, Ca, P, Fe, Ti, Mn. With exception of Pb, which was counted between 160–320 s all other elements were rated 10–50 s. Related 3 sigma detection limits were 0.025 wt.% (for Th), 0.023 wt.% (U), 0.011–0.015 wt.% (Pb) and <0.1 wt.% for all other elements. For acquisition of Pb an exponential background model was used. Details on the background modelling, analytical setting (element lines, crystals, and standards), detection limits and interference correction are given in Krenn et al. (2008).

Standards with contrasting U and Th concentrations were routinely used to control dead time adjustment and ZAF factors. As a further control of the analytical precision and the reliability of chemical dating, a monazite standard with well known age (341 ± 2 Ma, Friedl 1997) was routinely measured prior to and after 5 to 8 standard monazite analyses. In addition, standard monazites with Eo-Alpine and Proterozoic ages (~90 Ma, ~1385 Ma, ~1865 Ma) were also analysed together with the sample monazites.

Age and error calculations were carried out using the technique of Montel et al. (1996). Weighted average ages were calculated by internal error propagation (95% confidence) using Isoplot 2.49e (Ludwig 2001). Errors of the isochron ages were calculated using the least-squares fitting method of York (1966).

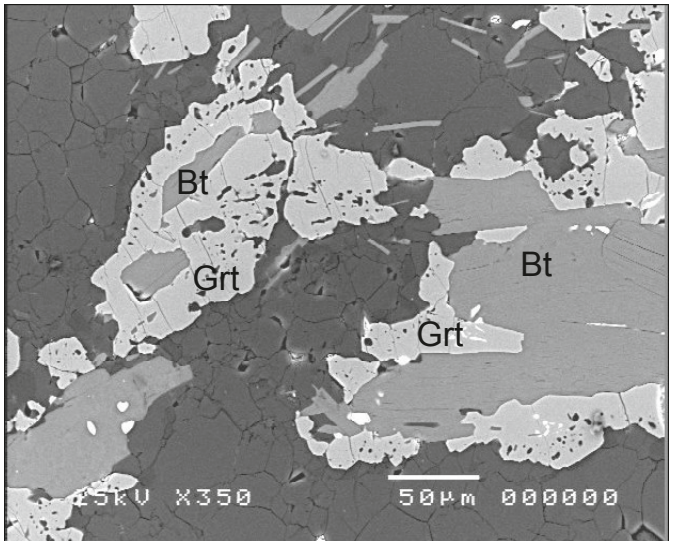

Fig. 8. BSE image from the Verpeil migmatite showing the formation of garnet around biotite (sample FB56E). Abbreviations: Grt = garnet, Bt = biotite. Note that garnet contains an inclusion-free inner rim and an inclusion-rich outer rim.

Confocal micro-Raman spectra were obtained with a HORIBA JOBIN YVON LabRam-HR 800 micro-Raman spectrometer. Samples were excited at room temperature with the 633 nm emission line of a 17 mW He-Ne-laser through an OLYMPUS 100X objective. The laser spot on the surface had a diameter of approximately 1 µm and a power of about 5 mW. Light was dispersed by a holographic grating with 1800 grooves/mm. Spectral resolution of about 1.8 cm^{-1} was experimentally determined by measuring the Rayleigh line. The dispersed light was collected by a 1024×256 open electrode CCD detector. Confocal pinhole was set to 1000 µm. Several spectra of single crystals of aluminium silicates in thin sections were recorded without polarizers for the exciting laser and the scattered Raman light. The spectra were baseline-corrected by subtracting linear or squared polynomial functions and fitted to Voigt functions. Peak shifts were calibrated by regular adjusting the zero-order position of the grating and controlled by measuring the Rayleigh line of a (100) polished single crystal silicon-wafer. Accuracy of Raman peak shifts was better than 0.5 cm^{-1}. The detection range was 100–4000 cm^{-1}.

Mineral chemistry

Garnet: Within the Winnebach migmatite polyphase garnet growth is evident in BSE images. The older garnets ($garnet_1$) (X_{Mg} = 0.07–0.09, X_{Fe} = 0.70–0.76, X_{Mn} = 0.12–0.13, X_{Ca} = 0.04–0.06) are almandine-rich with relatively constant Mg- and Mn-contents. The second generation ($garnet_2$) (X_{Mg} = 0.02–0.07, X_{Fe} = 0.52–0.56, X_{Mn} = 0.06–0.10, X_{Ca} = 0.25–0.26) forms grossular-rich rims around $garnet_1$ (Table 1, Fig. 3a). The garnets of the Verpeil migmatite are almandine-rich with high spessartine- and relatively low amounts of grossular- and pyrop components (X_{Mg} = 0.09, X_{Fe} = 0.6–0.62, X_{Mn} = 0.22–0.25, X_{Ca} = 0.01–0.02; Table 1, Fig. 8). Though two texturally different generations of garnet, an older, inclusion-free and a younger inclusion-rich garnet growing around biotite were detected, no chemical difference was observed. Garnet from the Nauderer Gaisloch migmatite shows a uniform composition of X_{Mg} = 0.08–0.11, X_{Fe} = 0.64–0.67, X_{Mn} = 0.20–0.23, X_{Ca} = 0.03–0.05 (Table 1).

Aluminium silicates: Two kyanite generations were identified in the Winnebach migmatite and the Nauderer Gaisloch migmatite using micro-Raman spectroscopy. The large, prismatic kyanites ($kyanite_1$) are chemically pure aluminium silicates. Fine-grained needles of kyanite 2 ($kyanite_2$) show evidence for Fe contents since they have a different micro-Raman spectrum showing fluorescence (Fig. 5c). These data are in agreement with the data of Klötzli-Chowanetz (2001) who identified two kyanite generations based on X-ray diffraction data. The fine-grained felt of $kyanite_2$ often occurs as a replacement product of $kyanite_1$ (Fig. 5a). Micro-Raman investigations on samples of the Verpeil migmatite also resulted in the identification of two generations of aluminium silicates, namely andalusite and kyanite, which can also be texturally discerned (Fig. 9). While kyanite forms larger prismatic crystals, andalusite appears as fine-grained aggregates. The large kyanite grains of the Nauderer Gaisloch migmatite contain 0.018 apfu Fe on average and therefore show a fluorescing Raman spectrum. The fine-grained kyanite felt within the muscovite-biotite-quartz aggre-

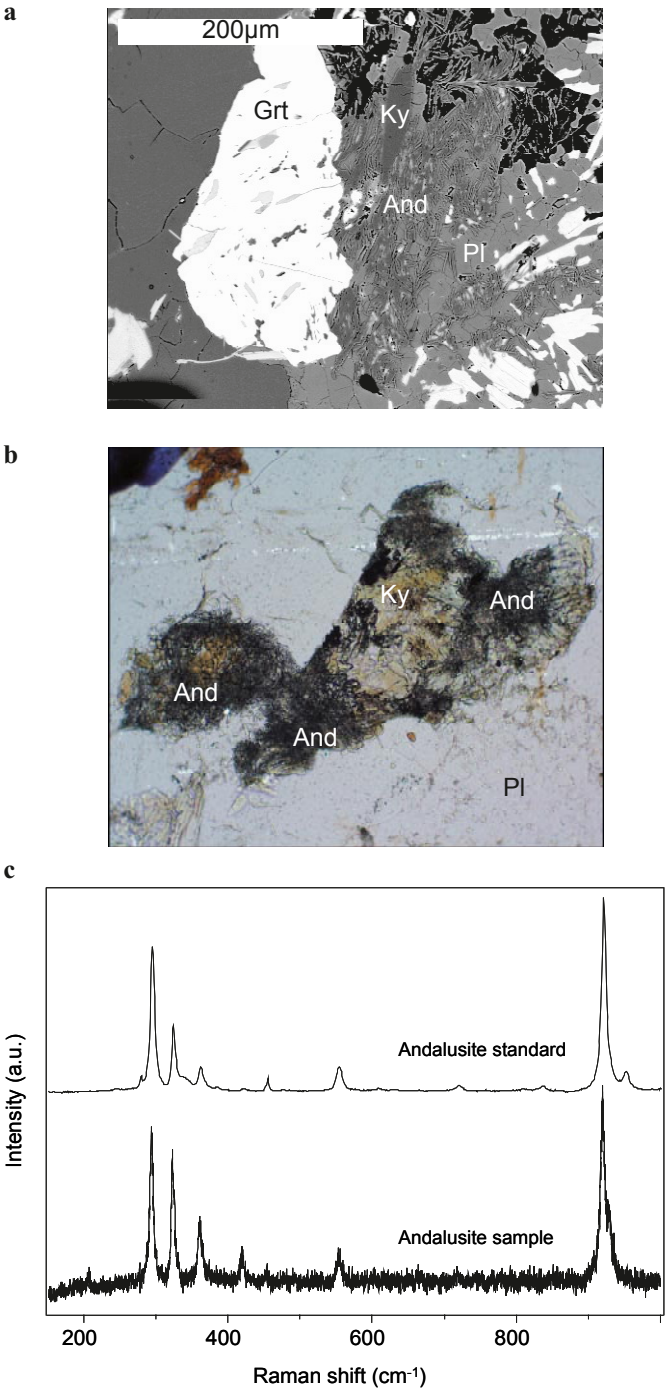

Fig. 9. a) BSE image of the Verpeil migmatite showing a large grain of kyanite surrounded by later formed andalusite adjacent to garnet (sample FB56E). (b): Microphotograph of a thin section from the Verpeil migmatite showing kyanite and later formed andalusite. (sample VP16, //P, length of bottom edge = 1.13 mm). c) Raman spectrum of andalusite from the Verpeil migmatite (sample FB56E).

Table 1. Representative electron microprobe analyses of garnet: Basis of formula calculation: 12 O and 8 cations; Fe3+ was calculated based on charge balance considerations. 1: garnet core (WB70); 2: garnet core (WB70); 3: garnet rim (WB49A); 4: garnet rim (WB49A); 5: garnet core (FB56A); 6: garnet rim (FB56A); 7: garnet core (NA50); 8: garnet rim (NA50);

Analysis	1	2	3	4	5	6	7	8
SiO_2	36.62	36.64	37.02	37.22	36.63	36.52	36.70	36.40
Al_2O_3	21.16	20.57	21.12	20.89	20.76	20.70	21.59	20.74
Fe_2O_3	1.82	0.55	1.81	3.05	1.29	1.42	1.20	1.55
FeO	29.96	31.58	24.58	22.70	27.35	27.03	28.99	28.37
MnO	5.31	5.51	2.97	2.67	9.49	10.38	10.00	8.37
MgO	1.88	1.79	1.51	1.76	2.29	2.21	1.90	2.62
CaO	3.27	2.70	10.92	11.88	2.15	1.71	0.91	1.57
∑	100.02	99.34	99.93	100.17	99.96	99.96	101.36	99.89
Si	2.954	2.993	2.953	2.947	2.969	2.966	2.946	2.953
Al	2.012	1.980	1.985	1.949	1.983	1.981	2.043	1.983
Fe^{3+}	0.110	0.034	0.109	0.182	0.078	0.087	0.073	0.095
Fe^{2+}	2.021	2.157	1.639	1.503	1.854	1.836	1.946	1.924
Mn	0.363	0.381	0.201	0.179	0.652	0.714	0.680	0.575
Mg	0.226	0.218	0.180	0.208	0.277	0.268	0.227	0.317
Ca	0.283	0.236	0.933	1.008	0.187	0.149	0.078	0.137
∑ Cat.	7.969	7.999	8.000	7.976	8.000	8.001	7.993	7.984
Mg#	0.075	0.072	0.059	0.068	0.091	0.088	0.076	0.104
Grossular	0.09	0.08	0.30	0.33	0.06	0.05	0.03	0.05
Almandine	0.67	0.71	0.53	0.49	0.61	0.60	0.64	0.63
Pyrope	0.08	0.07	0.06	0.07	0.09	0.09	0.08	0.10
Spessartine	0.12	0.13	0.07	0.06	0.21	0.23	0.23	0.19
Andradite	0.04	0.01	0.04	0.05	0.03	0.03	0.02	0.03

Table 2. Representative electron microprobe analyses of feldspars: Basis of formula calculations: 8 O and 5 cations; 1: plagioclase core (WB70); 2: plagioclase core (WB70); 3: plagioclase rim (WB43); 4: plagioclase (FB56A); 5: plagioclase (NA49a); 6: K-feldspar (VP16); 7: K-feldspar (WB70); 8: K-feldspar (NA49); n.d.: not detected

Analysis	1	2	3	4	5	6	7	8
SiO_2	64.17	63.58	64.30	62.85	68.35	64.06	62.63	63.29
Al_2O_3	20.83	22.49	20.22	23.50	20.08	18.72	19.54	18.89
CaO	2.26	3.26	1.62	4.36	0.38	0.16	n.d.	0.22
Na_2O	10.37	8.64	9.98	9.15	10.99	0.81	0.19	1.23
K_2O	0.13	0.31	0.23	0.34	n.d.	16.14	15.93	14.88
∑	98.65	98.64	96.35	100.54	99.80	99.89	98.29	98.51
Si	2.863	2.863	2.936	2.776	2.998	2.932	2.922	2.921
Al	1.095	1.194	1.088	1.219	1.038	1.009	1.074	1.028
Ca	0.108	0.157	0.079	0.206	0.018	0.008	n.d.	0.011
Na	0.897	0.754	0.884	0.781	0.935	0.072	0.017	0.110
K	0.007	0.018	0.013	0.019	n.d.	0.942	0.948	0.876
∑ Cat.	4.970	4.986	5.000	5.001	4.989	4.963	4.961	4.946
Albite	0.88	0.81	0.91	0.78	0.98	0.07	0.02	0.11
Anorthite	0.11	0.17	0.08	0.20	0.02	0.01	n.d.	0.01
K-feldspar	0.01	0.02	0.01	0.02	n.d.	0.92	0.98	0.88

gates shows a normal Raman spectrum but was too small for chemical analyses using the electron microprobe.

Plagioclase: Plagioclase is generally albite or oligoclase (Table 2). Plagioclase analyses of the Winnebach migmatite samples chemically show two generations similar to garnet. The Ca-rich cores (plagioclase$_1$; X_{Ca} = 0.11–0.16, X_{Na} = 0.81–0.89, $X_K \leq 0.02$) of the plagioclase are attributed to an older metamorphic event together with the Fe/Mn-rich garnet cores. The Na-rich rims of the plagioclase (plagioclase$_2$; X_{Ca} = 0.08, X_{Na} = 0.91–0.92, $X_K \leq 0.01$) and the Ca-rich rims of the garnet represent a younger metamorphic event. The plagioclase compositions from the Verpeil migmatite are uniform with X_{Ca} = 0.20–0.22, X_{Na} = 0.78, $X_K \leq 0.02$. Plagioclase from the Nauderer Gaisloch shows X_{Ca} = 0.02–0.05, X_{Na} = 0.95–0.98, $X_K \leq 0.01$.

K-feldspar: K-feldspar analyses from the Verpeil migmatite show $X_K = 0.88–0.92$, $X_{Na} = 0.07–0.11$, $X_{Ca} \leq 0.01$ and analyses from the Winnebach migmatite show compositions of $X_K = 0.98–1.00$, $X_{Na} \leq 0.02$. The K-feldspar compositions of the Nauderer Gaisloch migmatites are very similar to the samples from the Verpeil migmatite and are $X_K = 0.88$, $X_{Na} = 0.11$, $X_{Ca} = 0.01$ (Table 2).

Biotite: Although biotites from the Winnebach migmatite appear as two texturally different generations, chemically they are identical (Fe = ~1.30 apfu, Mg = 1.15 apfu, Ti = ~0.13 apfu). Biotites from the Verpeil migmatite show Fe = 1.28 apfu, Mg = 1.1 apfu and Ti = 0.15 apfu. Biotites of the Nauderer Gaisloch migmatite are also not zoned and show Ti contents between 0.1–0.18 apfu. Fe is around 1.25 apfu and Mg is between 0.95 and 1.05 apfu (Table 3).

Muscovite: White mica analyses from the three migmatite bodies show very similar results indicating a slight Tschermak's substitution which is most distinct in the Winnebach migmatite. White mica from the Winnebach migmatite shows Si = 3.19 apfu and Al = 2.43 apfu. The mica analyses from the other two migmatites show Si = 3.02–3.06 apfu and Al = 2.77–2.78 apfu. The celadonite component (Si – 3) is around 0.19 for the Winnebach migmatite and between 0.10 and 0.04 for the Verpeil migmatite. The Nauderer Gaisloch migmatite shows the lowest celadonite component of around 0.02 (Table 4).

Cordierite: Within the samples of the Verpeil migmatite cordierite is the only relict of a pre-Variscan metamorphic event.

Table 3. Representative electron microprobe analyses of biotite: Basis of formula calculations: 11 O; 1: biotite (WB70); 2: biotite (WB70); 3: biotite (FB56A); 4: biotite (FB56A); 5: biotite (NA49a); 6: biotite (NA49a); n.d.: not detected.

Analysis	1	2	3	4	5	6
SiO_2	34.48	35.13	36.03	35.80	35.34	35.33
TiO_2	1.74	1.61	0.28	0.13	2.40	2.27
Al_2O_3	19.46	19.08	21.48	21.22	20.24	20.17
FeO	21.31	21.30	16.91	18.06	18.30	18.90
MnO	0.29	n.d.	n.d.	0.32	0.42	0.43
MgO	9.21	9.27	11.18	11.35	9.14	9.02
Na_2O	n.d.	0.21	n.d.	n.d.	n.d.	0.29
K_2O	9.15	9.51	9.96	9.45	9.47	9.16
H_2O	3.92	3.94	4.02	4.03	4.50	3.88
Σ	99.68	100.17	99.86	100.47	99.75	99.80
Si	2.639	2.675	2.685	2.665	2.694	2.679
Ti	0.100	0.092	0.016	0.007	0.138	0.129
Al	1.713	1.713	1.887	1.862	1.819	1.803
Fe^{2+}	1.364	1.357	1.054	1.125	1.167	1.199
Mn	0.019	n.d.	n.d.	0.020	0.027	0.028
Mg	1.051	1.052	1.242	1.260	1.003	1.020
Na	n.d.	0.031	n.d.	n.d.	n.d.	0.043
K	0.893	0.924	0.947	0.898	0.921	0.917
H	2.000	2.000	2.000	2.000	2.000	2.000
Σ Cat.	7.830	7.847	7.830	7.845	7.783	7.809
Mg#	0.435	0.437	0.541	0.528	0.462	0.459

Table 4. Representative electron microprobe analyses of muscovite: Basis of formula calculations: 11 O; 1: muscovite (WB54); 2: muscovite (WB54); 3: muscovite (FB56A); 4: muscovite (FB56A); 5: muscovite (NA49a); 6: muscovite (NA49a); n.d.: not detected

Analysis	1	2	3	4	5	6
SiO_2	47.82	47.25	46.64	45.78	45.67	45.56
TiO_2	0.26	0.50	0.30	0.11	0.78	0.78
Al_2O_3	30.52	30.52	34.81	35.74	36.00	36.54
FeO	3.11	2.42	1.51	1.47	1.14	1.20
MgO	2.21	1.92	0.88	0.88	0.56	0.78
Na_2O	0.22	0.19	0.34	0.41	0.40	0.44
K_2O	11.33	11.35	10.87	11.39	11.01	10.78
H_2O	4.49	4.43	4.51	4.52	3.94	3.82
Σ	99.96	98.58	99.86	100.30	99.50	99.90
Si	3.193	3.195	3.098	3.039	3.022	2.995
Ti	0.013	0.025	0.015	0.006	0.046	0.039
Al	2.402	2.432	2.725	2.796	2.807	2.831
Fe^{2+}	0.156	0.123	0.076	0.073	0.057	0.059
Mg	0.220	0.194	0.087	0.087	0.055	0.076
Na	0.029	0.025	0.044	0.053	0.051	0.056
K	0.965	0.979	0.921	0.964	0.929	0.904
H	2.000	2.000	2.000	2.000	2.000	2.000
Σ Cat.	6.978	6.973	6.966	7.018	6.967	6.960

Table 5. Representative electron microprobe analyses of cordierite: Basis of formula calculations: 18 O + OH; Fe^{3+} was calculated based on charge balance considerations; 1–4: cordierite (FB56E).

Analysis	1	2	3	4
SiO_2	47.90	48.13	48.40	48.47
Al_2O_3	32.39	32.71	32.96	31.69
FeO	7.54	7.32	6.90	7.30
MnO	0.28	0.20	0.44	0.19
MgO	7.45	7.21	7.54	7.94
Na_2O	1.08	0.91	1.16	0.98
K_2O	0.05	0.08	0.02	0.05
Σ	96.69	96.56	97.42	96.62
Si	5.012	5.031	5.007	5.066
Al	3.995	4.030	4.019	3.903
Fe^{2+}	0.659	0.641	0.597	0.638
Mn	0.025	0.017	0.038	0.017
Mg	1.162	1.123	1.163	1.236
Na	0.219	0.186	0.232	0.198
K	0.006	0.009	0.002	0.007
Σ Cat.	11.078	11.037	11.058	11.065
Mg#	0.638	0.637	0.661	0.659

Strongly pinitized grains of cordierite could be measured and yielded $X_{Mg} = 0.64–0.66$ (Table 5).

Discussion

Textural relations between mineral assemblages and the sequence of metamorphic overprints

Since these migmatites underwent three metamorphic events, a pre-Variscan high-T, a Variscan medium P-T amphibo-

lite-facies, and a weak, Eo-Alpine, greenschist-facies overprint, and due to the fine-grained nature of the rocks and the development of subsequent mineral assemblages, detailed petrography involving the scanning electron microscope was performed to identify equilibrium mineral assemblages and attribute them to the metamorphic events. It is well known that in the case of the ÖC, the dominant mineral assemblages can be attributed to the Variscan metamorphic event and that the Eo-Alpine metamorphic overprint increases from NW to SE (e.g. Hoinkes et al. 1997; Neubauer et al. 1999). According to the metamorphic map of the ÖC, the Winnebach migmatite shows a strong Eo-Alpine metamorphic overprint since it is in the vicinity of the chloritoid-in isograd and the other two migmatites show a greenschist-facies metamorphic overprint. In the case of the Winnebach migmatite, the minerals plagioclase$_{1,2}$ + K-feldspar + garnet$_{1,2}$ + pinites + biotite + kyanite$_{1,2}$ + zircon + apatite + muscovite + chloritoid + quartz are present. We interpret garnet cores (garnet$_1$) as being part of the Variscan mineral assemblage while the Ca-rich rims (garnet$_2$) are attributed to the Eo-Alpine metamorphic event. Pre-Variscan cordierite, which occurs only as pinite relicts, could have formed by the model reaction:

Biotite + Sillimanite = Cordierite + K-feldspar + Melt (4)

During the Variscan event garnet$_1$ + kyanite$_1$ + plagioclase$_1$ + biotite formed, which led to the transformation of cordierite into kyanite and biotite by reactions such as (3) and into garnet$_1$ by reactions such as:

Cordierite + Biotite = Garnet + K-feldspar + H_2O (5)

No association of kyanite and crystallized melt domains could be observed and we propose that kyanite formed later, most probably during the Variscan metamorphic event, which also led to the formation of amphibolite-facies staurolite (Chowanetz 1991). This interpretation is in contrast to Klötzli-Chowanetz (2001) who attributed kyanite formation to the migmatization. During the Eo-Alpine metamorphic event garnet$_2$ (Ca-rich) + plagioclase$_2$ (Na-rich) + kyanite$_2$ + biotite + chloritoid formed in small microdomains along former fractures.

The mineral assemblage in the Verpeil migmatite was also determined by SEM and micro-RAMAN spectroscopy and is: K-feldspar + plagioclase + garnet + biotite + muscovite + cordierite + andalusite + kyanite + clinozoisite + zircon + apatite + rutile + quartz. Cordierite is interpreted to be the only remaining pre-Variscan relict. The dominant Variscan mineral assemblage is garnet + biotite + kyanite + K-feldspar + quartz. Again, cordierite most likely reacted to form garnet, biotite and kyanite by model reactions (3) and (5) as shown in Figures 7a–c. Andalusite formed during the retrograde Variscan evolution as described further south by Tropper & Hoinkes (1996). The Eo-Alpine mineral assemblage is chlorite + muscovite + albite, consistent with the Eo-Alpine greenschist-facies conditions in this area (Hoinkes et al. 1997).

The mineral assemblage of the Nauderer Gaisloch migmatite is garnet + quartz + biotite + plagioclase + muscovite + kyanite$_{1,2}$. In contrast to Verpeil, no relict cordierite is present anymore and only pseudomorphs after cordierite containing biotite and kyanite occur. Kyanite$_1$, which occurs as large grains in the matrix, was probably formed during the Variscan event, which also led to the transformation of cordierite into pseudomorphs containing biotite + kyanite$_2$ according to reaction (3) where kyanite$_2$ occurs as small needles (Fig. 10).

Thermobarometry

Multi-equilibrium calculations: The simultaneous calculation of all possible reactions within a defined chemical system has been done by using the program THERMOCALC v. 2.7 (Holland 1999, written comm.) and the data set of Holland & Powell (1998). The natural composition of coexisting minerals is taken into account using the activity models for garnet, plagioclase, muscovite and biotite from the set of proposed activity models from the program MacAX (Holland 1999, written comm.).

Inverse equilibrium approach (WEBINVEQ): In this approach, by giving the activities of the end-members of the coexisting minerals, a least squares estimate of the pressure and temperature of the equilibration of a mineral assemblage is calculated, based on the activities of the participating phases. Instead of using a set of independent equilibria, P and T estimates are found by finding the best-fit hyperplane to the partial molar free energies of all phase components. The basic principles of the method are described by Gordon (1992).

Pseudosections: Equilibrium phase diagrams for unmelted protolith paragneiss samples adjacent to the leucosomes, with the given bulk-rock composition were calculated in the chemical system SiO_2–TiO_2–Al_2O_3–FeO–MnO–MgO–CaO–Na_2O–

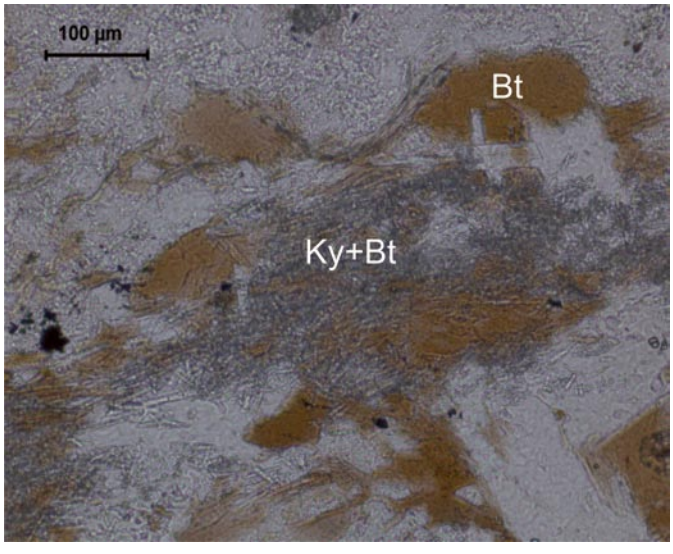

Fig. 10. Photograph of a thin section of sample NA49a from the Nauderer Gaisloch migmatite showing the intergrowth of biotite and kyanite (//P).

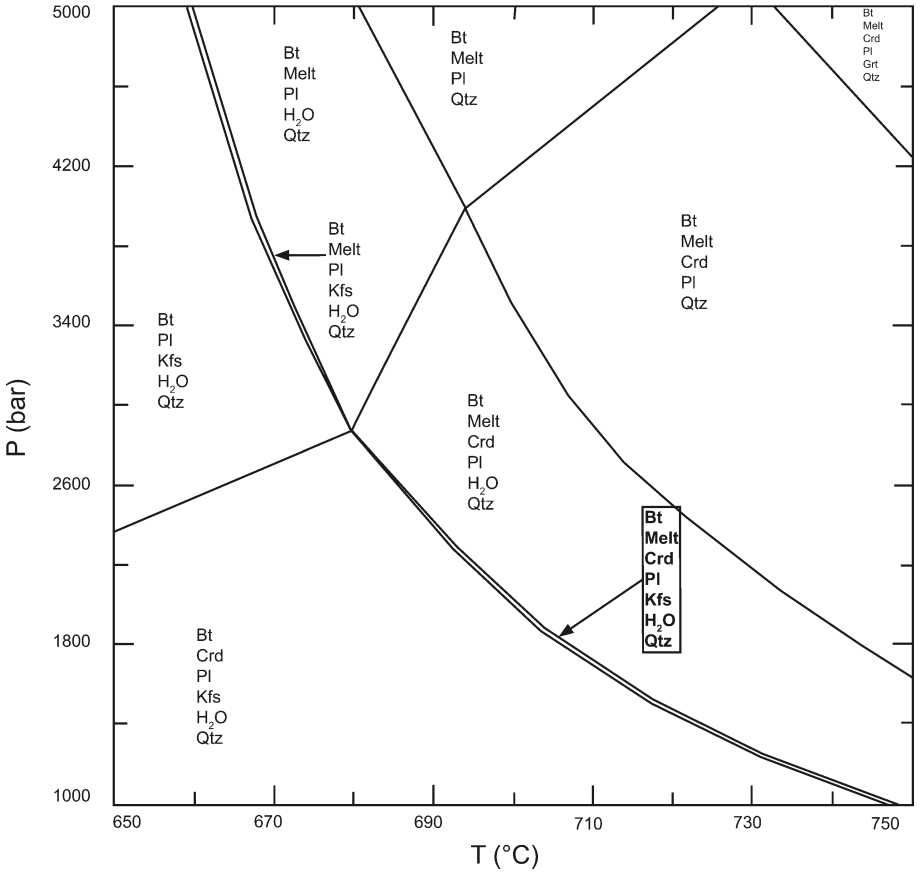

Fig. 11. Pseudosection calculated for sample VP2b from the Verpeil migmatite. The boxed assemblage biotite + cordierite + plagioclase + K-feldspar + melt + quartz is the observed mineral assemblage in the migmatite and is stable over a T-range of 670–750 °C and <2.8 kbar. Abbreviations: Crd: cordierite, Bt: biotite, Kfs: K-feldspar, Pl: plagioclase, Qtz: quartz.

K_2O–H_2O with the software PerpleX (Connolly 2005, written comm.) and the thermodynamic database of Holland & Powell (1998).

In addition to the programs discussed above, conventional thermobarometry using Fe-Mg exchange reactions and net-transfer equilibria was done with the program P-T-t-path by Spear & Kohn (1999 written comm.). For temperature calculations the garnet – biotite thermometer with the calibrations of Kleemann & Reinhardt (1994), Patiño Douce (1993), Perchuk & Lavrent'eva (1983) and Ferry & Spear (1978) with Berman (1990) were used. Pressure calculations were done with the the garnet – kyanite – plagioclase – quartz (GASP) barometer with the calibration of Koziol & Newton (1989) and the garnet – plagioclase – biotite – muscovite barometer using the calibration of Chun-Ming Wu (2004).

Pre-Variscan thermobarometry

Verpeil migmatite: The P-T conditions for this event were calculated with a pseudosection for a biotite-plagioclase host rock sample with the bulk-rock composition of SiO_2 = 77.51, TiO_2 = 0.61, Al_2O_3 = 11.17, Fe_2O_3 = 2.43, MnO = 0.05, MgO = 1.42, CaO = 1.99, Na_2O = 2.99, K_2O = 1.62, P_2O_5 = 0.19, Total = 99.96 and LOI = 1.11. The calculations yielded about 670–750 °C and pressures <2.8 kbar for the maximal baric stability of the assemblage biotite + cordierite + plagioclase + K-feldspar + quartz + melt as shown in Figure 11. These low P estimates also indicate that garnet was not stable during the high-T event.

Winnebach migmatite: Textural evidence from the Winnebach migmatite shows that during the pre-Variscan event the water saturated granite solidus was overstepped indicating temperatures of at least 650 °C at pressures <5 kbar (Boettcher & Wyllie 1968). Hoinkes (1973) experimentally obtained temperatures of 685 °C and pressures ≥4 kbar for the pre-Variscan event. Similar P-T conditions as for the Verpeil migmatite were also calculated using the composition of a biotite-plagioclase host rock sample from the Winnebach migmatite given by Hoinkes et al. (1972). The obtained pressure estimates of <2.8 kbar are also in agreement with the petrogenetic grid of Spear et al. (1999) since the presence of K-feldspar in the leucosomes indicates pressures <4 kbar, which is also consistent with the absence of garnet during migmatization. In contrast to these data, Klötzli-Chowanetz (2001) assumes partial anatexis in the kyanite stability field, since she interprets $kyanite_1$ to be a product of anatectical reactions above the invariant point of the system KASH, which is above 4 kbar and hence attributes $kyanite_1$ to be of pre-Variscan origin. She assumes that $garnet_1$ is also of pre-Variscan origin and in combination with the petrogenetic grid of Spear et al. (1999) this indicates pressures of at least 7–8 kbar for the partial anatexis.

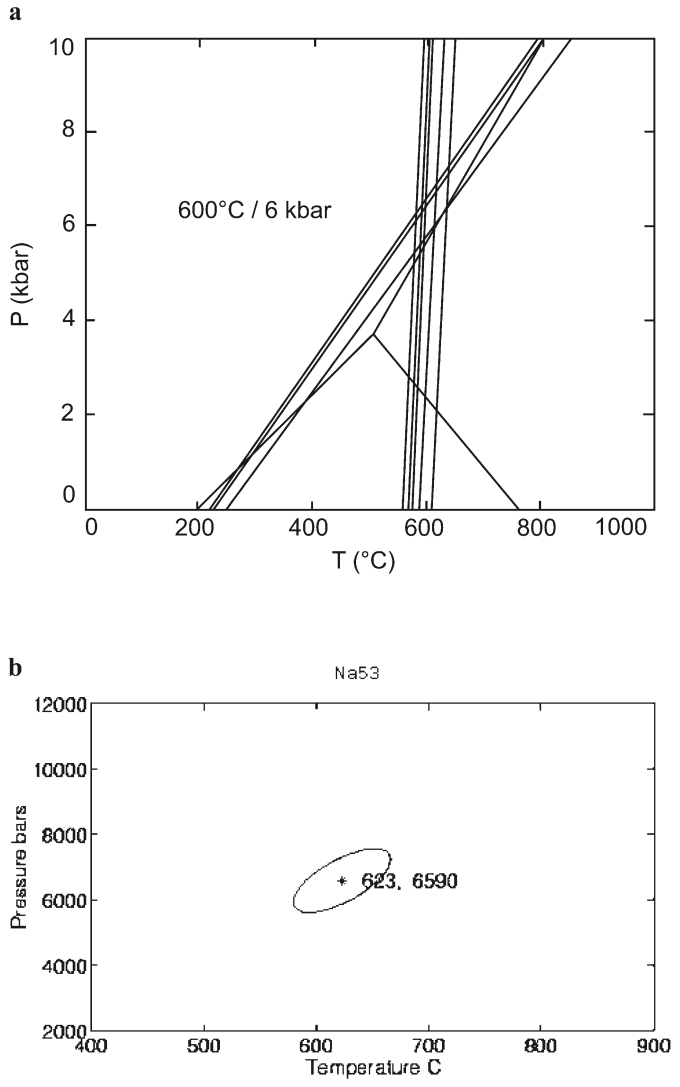

Fig. 12. a) Variscan P-T conditions of the Verpeil migmatite calculated with the program P-T-t-path (sample VP16). b) Variscan P-T conditions of the Nauderer Gaisloch migmatite calculated with the program WEBINVEQ (sample NA 53).

Variscan thermobarometry

Verpeil migmatite: Garnet-biotite temperatures from the Verpeil migmatite range from 470 to 650 °C (at 5 kbar). The most uniform data set were obtained using the calibration of Kleemann & Reinhardt (1994), which yielded 530–600 °C. The highest results were obtained with the calibration Patiño Douce (1993) and yielded approximately 660 °C. The lowest temperatures were calculated with the calibration of Ferry and Spear (1978) with the garnet activity model of Berman (1990). The calibration of Perchuk & Lavrent'eva (1983) also yielded uniform temperatures of 580–615 °C for garnet-biotite pairs from the Verpeil migmatite. Calculation with THERMOCALC v 2.7 yielded the following reactions for the equilibrium assemblage garnet + plagioclase + K-feldspar + quartz:

Phlogopite + Anorthite
= Pyrope + Grossular + Eastonite + Quartz (6)

Phlogopite + Annite + Anorthite
= Grossular + Almandine + Eastonite + Quartz (7)

Pyrope + Annite + Anorthite =
Grossular + Almandine + Eastonite + Quartz (8)

Almandine + Phlogopite = Pyrope + Annite (9)

Due to the small grossular component in the garnets, the P-estimates have to be treaded with caution (Todd 1998). Nonetheless, these calculations yield P-T conditions of 6–7 kbar and 550–650 °C. These data are in very good agreement with the data of Tropper & Hoinkes (1996), who calculated metamorphic conditions of 600–640 °C and 5–6 kbar for the Variscan event in the western ÖC. Calculations with the program P-T-t-path using the garnet – biotite thermometer and the garnet – kyanite – plagioclase – quartz (GASP) barometer yielded the same P-T conditions of 600 °C and 6 kbar (Fig. 12a). Calculations using WEBINVEQ yielded 5.8 ± 0.7 kbar and 612 ± 32 °C.

Winnebach migmatite: Garnet-biotite thermometry, using the calibration of Perchuk & Lavrent'eva (1983) yielded temperatures of 580–620 °C (at 5 kbar), which is a much smaller temperature range than from Chowanetz (1991) and Klötzli-Chowanetz (2001) who obtained temperatures of 480–700 °C for the Variscan event. Calculation with the program THERMOCALC resulted in the following reactions using the mineral assemblage garnet$_1$ + biotite + plagioclase$_1$ + K-feldspar + quartz:

Phlogopite + Anorthite + Quartz
= Pyrope + Grossular + Sanidine + H_2O (10)

Pyrope + Grossular + Muscovite
= Phlogopite + Anorthite (11)

Grossular + Muscovite + Quartz
= Anorthite + Sanidine + H_2O (12)

Phlogopite + Muscovite + Quartz
= Pyrope + Sanidine + H_2O (13)

The intersection of these reactions yielded P-T conditions of 5.7 ± 2.6 kbar and 676 ± 56 °C.

Nauderer Gaisloch migmatite: Calculations with the program P-T-t-path using the garnet biotite thermometer, the GASP barometer and the garnet – plagioclase – biotite – muscovite barometer according to reaction (11) using the calibration of Chun-Ming Wu (2004), resulted in P-T conditions of 550–570 °C and 4–7 kbar. Calculations with WEBINVEQ resulted in a temperature range of 500–650 °C and pressures of 5–6.5 kbar (Fig. 12b). THERMOCALC v 2.7 yielded similar conditions of 610–660 °C and 5.1–5.3 kbar.

Eo-Alpine thermobarometry

Calculation of the Eo-Alpine P-T conditions was only attempted in the Winnebach migmatite. For these calculations, the assemblage garnet$_2$ (Ca-rich rims) + plagioclase$_2$ (albite-rich rims) + biotite (small grains adjacent to Ca-rich garnet$_2$, Fig. 4) + kyanite + quartz + chloritoid was used. The calculations using the program P-T-t-path yielded P-T conditions of 485 °C and 8.5 kbar as shown in Figure 13. These results are in agreement with thermobarometric results from this area (Tropper & Recheis 2003). Calculations with THERMOCALC v 2.7 resulted in pressures of 8.6 ± 0.2 kbar and slightly lower temperatures of 433 ± 12 °C.

Geochronology

U-Th-Pb electron microprobe dating of monazites from three samples from the leucosome of the Winnebach migmatite yielded ages ranging from 408 ± 46 Ma to 472 ± 36 Ma for the partial anatexis as shown in Table 6. These ages show a higher spread and are also slightly younger than previously reported ages from the Winnebach migmatite which were around 490 Ma (Klötzli-Chowanetz 2001). The geochronological data from monazites of four leucosome samples from the Verpeil migmatite range from 409 ± 50 Ma to 457 ± 42 Ma for the anatectic event, which is similar within the error with the data obtained from the Winnebach migmatite. Geochronological investigations on monazites from two leucosome samples of the Nauderer Gaisloch migmatite resulted in ages ranging from 431 ± 37 Ma to 472 ± 31 Ma (Fig. 14), again in good agreement with the data from the other two migmatites. In addition, a second generation of monazite which formed during the subsequent Variscan metamorphic event was detected. These grains yielded ages ranging from 305 ± 43 Ma to 336 ± 42 Ma (Table 6; Fig. 14).

Discussion

Although our P-T data of the pre-Variscan migmatization yield somewhat lower pressures of <2.8 kbar than previous investigations, the data are in agreement with petrogenetic grids and textural observations. Hoinkes (1973) estimated the P-T conditions of the migmatization, based on experiments, to be 660–685 °C and ≥4 kbar. Söllner et al. (1982) obtained similar P-T results by using petrogenetic grids from the literature. Klötzli-Chowanetz et al. (2001) deduced significantly higher pressures and temperatures of 8 kbar and ca. 750 °C for the anatexis based on petrographic evidence and comparison to the petrogenetic grid by Spear et al. (1999). The latter pressure estimates strongly depend on the interpretation of kyanite as being present during anatexis, which could not be verified in our investigation.

Previous thermobarometric investigations of the Variscan P-T conditions by Veltman (1986), Tropper & Hoinkes (1996), and Tropper & Recheis (2003) from the ÖC yield P-T conditions of 570–750 °C and 5.8–8 kbar. Veltman (1986) obtained from the northern kyanite zone 570–650 °C and 4.3–7.8 kbar. For the sillimanite zone, he reported P-T conditions of 600–750 °C and 4.2–6.8 kbar. Tropper & Hoinkes (1996) obtained 570–640 °C and 5.8–7.5 kbar for the central andalusite zone and Tropper & Recheis (2003) obtained P-T conditions of 469–630 °C and 4.2–7.3 kbar for the northern kyanite zone and 578 °C and 7.2 kbar for the southern kyanite zone. The data from the Verpeil- and the Nauderer Gaisloch migmatites are well in accordance with these results, only the temperatures of the Winnebach migmatite are slightly lower, thus possibly indicating a later Eo-Alpine rejuvination.

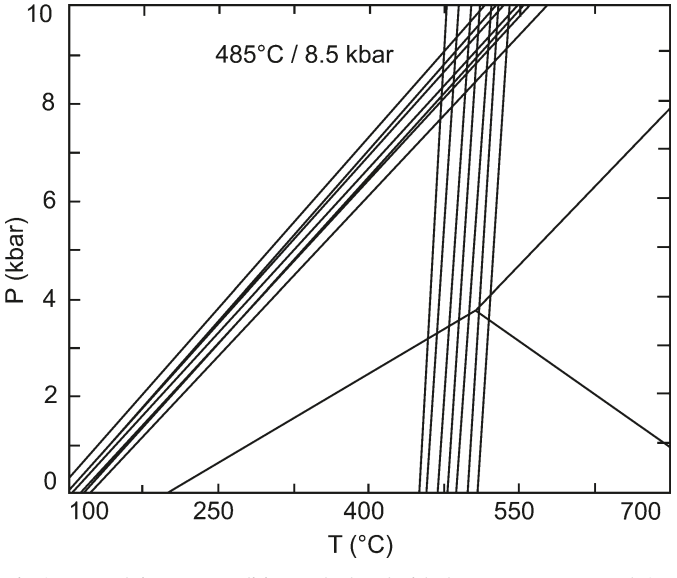

Fig. 13. Eo-Alpine P-T conditions calculated with the program P-T-t-path for the Winnebach migmatite (sample WB 70).

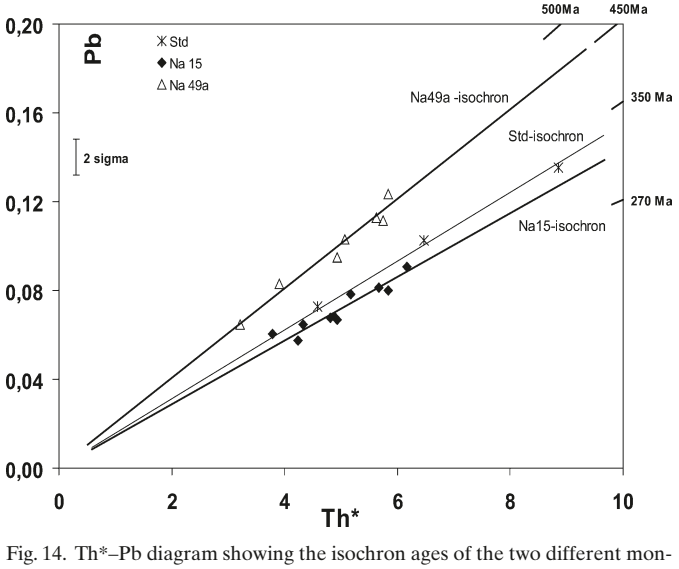

Fig. 14. Th*–Pb diagram showing the isochron ages of the two different monazite generations from the Nauderer Gaisloch migmatite (samples Na49a, Na15). Na49a (open triangles) yields pre-Variscan ages and Na15 (black diamonds) Variscan ages as discussed in the text.

Table 6. U-Th-Pb electron microprobe analyses data of monazites: Th. U and Pb contents. Th* values (Suzuki et al. 1991) and chemical ages (calculated after Montel et al. 1996) of monazites from samples WB70B1, WB29/2, VP28, FB56A, NA15, NA49. Errors are 2σ for the single points and at the 95% confidence level for the weighted average age.

	Y	Th	U	Pb	Th*	Age	Error (2σ)	
WB 70 B1 Mon1	1,306	3,702	0,371	0,095	4,917	433	33	
WB 70 B1 Mon2	1,304	3,525	0,780	0,116	6,081	426	27	
WB 70 B1 Mon3	1,268	3,822	0,241	0,098	4,614	472	36	MSWD = 1.8
WB 70 B1 Mon4	1,702	3,821	1,245	0,164	7,911	463	21	
WB 70 B1 Mon5	1,515	3,759	0,401	0,100	5,073	441	32	
WB 29/2 Mon1	1,639	3,702	0,943	0,138	6,798	455	27	
WB 29/2 Mon2	1,627	3,485	0,985	0,132	6,716	442	27	
WB 29/2 Mon3	1,387	2,246	0,602	0,084	4,219	444	43	
WB 29/2 Mon4	1,038	2,548	0,501	0,086	4,192	457	43	MSWD = 0.74
WB 29/2 Mon5	1,282	2,174	0,544	0,072	3,953	408	46	
WB 29/2 Mon6	1,141	3,203	0,371	0,087	4,418	438	41	
VP 28 Mon1	1,335	2,121	0,353	0,060	3,275	409	50	
VP 28 Mon2	1,616	1,765	0,664	0,080	3,945	457	42	
VP 28 Mon3	1,204	4,280	0,428	0,115	5,685	452	29	MSWD = 1.6
VP 28 Mon4	0,824	3,937	0,314	0,101	4,969	456	33	
VP 28 Mon5	1,189	2,809	0,421	0,076	4,185	408	39	
FB 56A Mon1	1,763	3,726	0,729	0,118	6,114	433	30	
FB 56A Mon2	2,056	7,259	0,781	0,200	9,824	454	18	
FB 56A Mon3	1,881	3,530	0,759	0,115	6,015	427	30	
FB 56A Mon4	1,127	2,332	0,280	0,061	3,249	419	56	MSWD = 1.6
FB 56A Mon5	1,749	3,214	1,379	0,143	7,728	416	24	
FB 56A Mon6	1,927	3,591	1,532	0,164	8,610	428	21	
NA 15 Mon1	1,968	2,887	0,615	0,068	4,885	313	37	
NA 15 Mon2	2,204	3,056	0,652	0,079	5,178	340	35	
NA 15 Mon3	2,056	2,606	0,678	0,068	4,807	316	38	
Na 15 Mon4	2,231	3,788	0,632	0,080	5,838	308	31	
NA 15 Mon5	1,531	4,329	0,566	0,091	6,169	330	29	
NA 15 Mon6	1,882	2,343	0,611	0,065	4,329	336	42	MSWD = 0.75
NA 15 Mon7	1,978	2,848	0,641	0,067	4,928	305	37	
NA 15 Mon8	1,697	2,311	0,454	0,061	3,791	358	48	
NA 15 Mon9	1,886	3,392	0,702	0,081	5,674	321	32	
NA 15 Mon10	1,967	2,088	0,662	0,057	4,237	305	43	
NA 49 Mon1	1,036	2,053	0,355	0,065	3,217	449	56	
NA 49 Mon2	1,137	2,705	0,364	0,083	3,901	475	46	
NA 49 Mon3	1,484	3,242	0,517	0,095	4,935	431	37	
NA 49 Mon4	1,424	3,516	0,471	0,103	5,061	455	36	MSWD = 0.88
NA 49 Mon5	1,736	4,310	0,464	0,123	5,836	472	31	
NA 49 Mon6	1,536	3,993	0,536	0,112	5,749	435	31	
NA 49 Mon7	1,331	4,054	0,480	0,113	5,630	448	32	

The Eo-Alpine P-T conditions of this investigation from the Winnebach migmatite agree with P-T estimates of the chloritoid-in isograd of 421–495 °C and 6.7–9.4 kbar for samples from the Ortler-Campo Crystalline Complex (Mair et al. 2006) as well as with the Eo-Alpine P-increase from NW to SE (e.g. Veltman 1986; Tropper & Recheis,2003).

Although the obtained U-Th-Pb ages of monazite cluster around 430–450 Ma in all three migmatites and thus confirm a pervasive pre-Variscan event throughout the ÖC, which has not been confirmed yet, still large discrepancies concerning previously published age data remain. Söllner & Hansen (1987) and Söllner (2001) obtained Pan-African ages of 607–670 Ma on zircons, which they interpret as the age of the anatexis. Klötzli-Chowanetz et al. (1997) obtained an age of the migmatization of 490 ± 9 Ma and minimum cooling ages, based on Rb-Sr isochron ages of muscovite, of 461 ± 4 Ma (Chowanetz 1991; Klötzli-Chowanetz 2001). On the other hand, even the age of the pre-Variscan event in the Winnebach migmatite is still not unambiguous since Klötzli-Chowanetz et al. (1997) also provided some evidence for even older thermal events at 560 Ma and 635 Ma. Similarly, highly variable pre-Variscan ages have also been obtained from the Nauderer Gaisloch migmatite, which yielded several stages of zircon growth, namely 531 ± 11 Ma, which is thought to be the age of the anatexis, 585 ± 8 Ma (Pan-African), and 430 ± 6 Ma (Silurian high-T event). The age of the tonalite is constrained to be 487 ± 11 Ma and that of a pegmatite crosscutting the migmatites at the Nauderer Gaisloch is 472 ± 26 Ma (Klötzli-Chowanetz et al. 2001; Schweigl 1993). These data are also somewhat older than the ages we obtained from this migmatite complex (Table 6). The only ages that were

so far available from the Verpeil area are Rb-Sr ages from two different types of orthogneisses, which are in the vicinity of the migmatite body (Bernhard 1994). The first type, a hedenbergite-hornblende orthogneiss, shows a minimum intrusion age of 417 ± 9 Ma, which is similar to the age of the second type of intrusion, a hornblende-bearing tonalitic gneiss, which shows an age of 408 ± 20 Ma. Both ages are considerable younger than the ages of the monazites obtained in this study. The majority of intrusives in the central ÖC shows ages in the range between 420 and 485 Ma (Thöni 1999). These ages seem to correlate well with the monazite ages of the ÖC migmatites, thus placing a rather reliable time constraint on the formation of the migmatites during the early Ordovician.

Acknowledgments

The authors wish to thank the FWF for partial financial support in the course of project P17878-N10. Edgar Mersdorf and Bernhard Sartory are thanked for their help with the electron microprobe. The manuscript was considerably improved by the careful reviews of Thorsten Nagel and Igor Petrik. Niko Froitzheim is thanked for the editorial handling.

REFERENCES

Berman, R.G. 1990: Mixing properties of Ca-Mg-Fe-Mn garnets, American Mineralogist 75, 328–344.

Bernhard, F. 1994: Zur magmatischen und metamorphen Entwicklung im westlichen Ötztal-Stubai Kristallin (Bereich Feichten-Verpeil, mittleres Kaunertal). Unpublished Masters Thesis, University Graz, 314 pp.

Bernhard, F., Klötzli, U., Thöni, M. & Hoinkes, G. 1996: Age, origin and geodynamic significance of a polymetamorphic felsic intrusion in the Ötztal Crystalline Basement, Tirol, Austria. Mineralogy and Petrology 58, 171–196.

Boettcher, A.L. & Wyllie, P.J. 1968: Melting of granite with excess water to 30 kbar pressure. Journal of Geology 76, 235.

Chowanetz, E. 1991: Strukturelle und geochronologische Argumente für eine altpaläozoische Anatexis im Winnebachmigmatit (Ötztal/Tirol, Österreich). Mitteilungen der Gesellschaft der Geologie und Bergbaustudenten Österreichs 37, 15–36.

Cocherie, A., Mezeme, E.B., Legendre, O., Fanning, C.M., Faure, M. & Rossi, P. 2005: Electron-microprobe dating as a tool for determining the closure of Th-U-Pb system in migmatitic monazites. American Mineralogist 90, 607–618, 2005.

Drong, H-J. 1959: Das Migmatitgebiet des „Winnebachgranits“ (Ötztal-Tirol) als Beispiel einer petrotektonischen Analyse. Tschermaks Mineralogische Petrographische Mitteilungen 7, 1–69.

Ferry, J.M. & Spear, F.S. 1978: Experimental calibration of the partitioning of Fe and Mg between biotite and garnet. Contributions to Mineralogy and Petrology 66, 113–117.

Finger, F. et al. 1996: Altersdatierungen von Monaziten mit der Elektronenstrahlmikrosonde – Eine wichtige neue Methode in den Geowissenschaften. TSK 6, 118–122.

Finger, F., Broska, I., Roberts, M.P. & Schermaier, A. 1998: Replacement of primary monazite by apatite-allanite-epidote coronas in amphibolite facies granite gneiss from the eastern Alps. American Mineralogist 83, 248–258.

Finger, F. & Helmy, H. 1998: Composition and total-Pb model ages of monazite from high-grade paragneisses in the Abu Swayel area, southern Eastern Desert, Egypt. Mineralogy and Petrology 62, 269–289.

Goncalves, P., Nicollet, C. & Montel, J.M. 2004: Petrology and in situ U-Th-Pb Monazite Geochronology of Ultrahigh-Temperature Metamorphism from the Andriamena Mafic Unit, North-Central Madagascar. Significance of a Petrographical P-T Paths in a Polymetamorphic Context. Journal of Petrology 10, 1923–1957.

Gordon, T.M. 1992: Generalized thermobarometry: solution of the inverse chemical equilibrium problem using data for individual species. Geochimica et Cosmochimica Acta 56, 1793–1800.

Hammer, W. 1925: Cordieritführende metamorphe Granite aus den Ötztaler Alpen. Tschermaks Mineralogische Petrographische Mitteilungen 38, 67–87.

Hoinkes, G., Purtscheller, F. & Schantl, J. 1972: Zur Petrographie und Genese des Winnebachgranites (Ötztaler Alpen, Tirol). Tschermaks Mineralogische Petrographische Mitteilungen 18, 292–311.

Hoinkes, G. 1973: Die Anatexis des Winnebachgranites (Ötztaler Alpen, Österreich) am Beispiel eines Aufschlusses. Tschermaks Mineralogische Petrographische Mitteilungen 20, 225–239.

Hoinkes, G., Thöni, M., Bernhard, F., Kaindl, R., Lichem, C., Schweigl, J., Tropper, P. & Cosca, M. 1997: Metagranitoids and associated metasediments as indicators for the pre-Alpine magmatic and metamorphic evolution of the Western Austroalpine Ötztal Basement (Kaunertal, Tirol). Schweizerische Mineralogische und Petrographische Mitteilungen 77, 299–314.

Hoinkes, G., Koller, F., Rantitsch, G., Dachs, E., Höck, V., Neubauer, F. & Schuster, R. 1999: Alpine metamorphism of the Eastern Alps. Schweizerische Mineralogische Petrographische Mitteilungen 79, 155–181.

Holland, T.J. B. & Powell, R. 1998: An internally-consistent thermodynamic data set for phases of petrological interest. Journal of Metamorphic Geology 8, 89–124.

Jarosevich, E.J., Nelen, J.A. & Norberg, J.A. 1980: Reference samples for electron microprobe analysis. Geostandards Newsletter 4, 87–133.

Jarosevich, E.J. & Boatner, L.A. 1991: Rare earth element reference samples for electron microprobe analysis. Geostandards Newsletter 15, 397–399.

Jercinovich, M.J. & Williams, M.L. 2005: Analytical perils (and progress) in electron microprobe trace element analysis applied to geochronology: Background acquisition, interferences and beam irradiation effects. American Mineralogist 90, 526–546.

Kleemann, U. & Reinhardt, J. 1994: Garnet – biotite thermometry revisited; the effect of Al (super VI) and Ti in biotite. European Journal of Mineralogy 6, 925.

Klötzli-Chowanetz, E., Klötzli, U. & Koller, F. 1997: Lower Ordovician migmatization in the Ötztal crystalline basement (Eastern Alps, Austria): linking U-Pb and Pb-Pb dating with zircon morphology. Schweizerische Mineralogische Petrographische Mitteilungen 77, 315–324.

Klötzli-Chowanetz, E. 2001: Migmatite des Ötztalkristallins – Petrologie und Geochronologie. Unpublished PhD Thesis University of Vienna, 155 pp.

Koziol, A.M. & Newton, R.C. 1989: Grossular activity – composition relationships in ternary garnets determined by reversed displaced equilibrium experiments. Contributions to Mineralogy and Petrology 103, 423.

Mair, V., Tropper, P., Schuster, R. 2006: The P-T-t evolution of the Ortler-Campo Crystalline (South-Tyrol/Italy). PANGEO 2006, Innsbruck University Press, 186–187.

Mehnert, K.R. 1968: Migmatites and the origin of granitic rocks. Elsevir, Amsterdam.

Miller, C. & Thöni, M. 1995: Origin of eclogites from the Austroalpine Ötztal Basement (Tirol, Austia): geochemistry and Sm-Nd vs. Rb-Sr isotope systematics. Chemical Geology 137, 283–310.

Neubauer, F., Hoinkes, G., Sassi, F.P., Handler, R., Höck, V., Koller, F. & Frank, W. 1999: Pre-Alpine metamorphism in the Eastern Alps. Schweizerische Mineralogische Petrographische Mitteilungen 79, 41–62.

Ohnesorge, T. 1905: Die vorderen Kühtaier Berge. Verhandlungen der Geologischen Reichsanstalt Wien. Jahrgang 1905, 175–182.

Patiño Douce, A.E. 1993: Titanium substitution in biotite: an empirical model with applications to thermometry, O_2 and H_2O barometries, and consequences for biotite stability. Chemical Geology 108, 133–162.

Perchuk, L.L. & Lavrent'eva, I.V. 1983: Experimental investigations of exchange equilibria in the system cordierite – garnet – biotite. In: Saxena (Ed). Kinetics and Equilibrium in Mineral Reactions Berlin (Springer Verlag), 199–239.

Schindlmayer, A. 1999: Granitoids and plutonic evolution of the Ötztal-Stubai Massif: a key for understanding the Early Paleozoic history of the Austroalpine crystalline basement in the western Eastern Alps. Unpublished Ph.D. Thesis Universität Salzburg, 287 pp.

Schweigl, J. 1993: Kristallingeologische Untersuchungen in den Nauderer Bergen (Westliche Ötztaler Alpen, Tirol). Unpublished Masters Thesis Universität Wien, 87 pp.

Söllner, F., Schmidt, K., Bumann, A. & Hansen, B.T. 1982: Zur Altersstellung des Winnebach-Migmatits im Ötztal (Ostalpen). Verhandlungen der Geologischen Bundesanstalt 1982, 95–106.

Söllner, F. & Hansen, B.T. 1987: „Pan-afrikanisches“ und „kaledonisches“ Ereignis im Ötztal-Kristallin der Ostalpen: Rb-Sr- und U-Pb-Altersbestimmungen an Migmatiten und Metamorphiten. Jahrbuch der Geologischen Bundesanstalt 130/4, 529–569.

Söllner, F. 2001: The Winnebach migmatite (Ötz-Stubai crystalline unit) – evidence for a Pan-Africanic metamorphism in an overthrust nappe sequence in the Eastern Alps. Geologisch Paläontologische Mitteilungen der Universität Innsbruck 25, 199–200.

Spear, F.S., Kohn, M.J. & Cheney, J.T. 1999: P-T paths from anatectic pelites. Contributions to Mineralogy and Petrology 134, 17–32.

Thöni, M. 1999: A review of geochronological data from the Eastern Alps. Schweizerische Mineralogische Petrographische Mitteilungen 79, 209–230.

Todd, C.S. 1998: Limits on the precision of geobarometry at low grossular and anorthite content. American MIneralogist 83, 1161–1168.

Tropper, P. & Hoinkes, G. 1996: Thermobarometry in Al_2SiO_5-bearing metapelites in the western Austroalpine Ötztal-basement. Mineralogy and Petrology 58, 145–170.

Tropper, P. & Recheis, A. 2003: Garnet zoning as a window into the metamorphic evolution of a crystalline complex: the northern and central Austroalpine Ötztal-Complex as a polymorphic example. Mitteilungen der Österreichischen Geologischen Gesellschaft 94, 27–53.

Veltman, C. 1986: Zur Polymetamorphose metapelitischer Gesteine des Ötztal Stubaier Altkristallins. Unpublished Ph.D. Thesis Universität Innsbruck, 164 pp.

Williams, M.L., Jercinovic, M.J., Goncalves, P. & Mahan, K. 2006: Format and philosophy for collecting, compiling, and reporting microprobe monazite ages. Chemical Geology 225,1–15.

Wu, C.-M., Zhang, J. & Ren, L.-D. 2004: Empirical garnet – muscovite – plagioclase – quartz – geobarometry in medium- to high-grade metapelites. Lithos 78, 319.

Manuscript received January 18, 2008
Revision accepted June 3, 2008
Published Online first November 13, 2008
Editorial Handling: Nikolaus Froitzheim & Stefan Bucher